Matematisk-fysiske Meddelelser
udgivet af
Det Kongelige Danske Videnskabernes Selskab
Bind **34,** nr. 5

Mat. Fys. Medd. Dan. Vid. Selsk. **34,** no. 5 (1964)

STOPPING OF 50 keV IONS IN GASES

BY

N. O. LASSEN, N. O. ROY POULSEN, G. SIDENIUS
AND LISE VISTISEN

København 1964
Kommissionær: Ejnar Munksgaard

Synopsis

Ions of radioactive isotopes were from an isotope separator passed through a small hole into a chamber filled with a stopping gas at low pressure. The thermalized ions were collected by a transverse electric field; from studies of the activity distribution on the collector plates information was obtained about the charge state of the particles, and about the most probable and the mean range, the straggling, and the scattering. The results are compared to the theory by Lindhard, Scharff and Schiøtt.

Printed in Denmark
Bianco Lunos Bogtrykkeri A/S

1. Introduction

Measurements of the ranges of gallium ions of energies about one MeV were reported in a previous paper[1]. The results are in general agreement with a range formula given by LINDHARD and SCHARFF[2]. It was an interesting observation that the range R_D in deuterium is longer than the range R_H in hydrogen, a difference which must be ascribed to the influence of nuclear encounters. However, the relative difference $(R_D - R_H)/R_H$ seemed to decrease with decreasing ion energy; at first sight this is strange, since the nuclear stopping plays a larger role at smaller energies, but it is in accord with the result of HARVEY et. al.[3], who found a shorter range in deuterium than in hydrogen for Th-ions of a somewhat smaller velocity. In our previous investigations the lower limit for the accessible energy interval was about 0.5 MeV. It was desirable to study the ranges of Ga-ions at much smaller energy; the ratio R_D/R_H depends not only on the relative influence of nuclear and electronic stopping, but also on the more detailed behaviour of the former. When two ions meet in a close collision, the potential describing the force between them is not the simple r^{-1}-potential, because the nuclei are screened by the accompanying electrons. For low energy, where the energy loss due to electronic encounters may be neglected, the range in deuterium, according to LINDHARD and SCHARFF[4], will be longer or shorter than the range in hydrogen, depending on whether the screened potential varies slower or faster than r^{-2}. Recently, a more detailed theory for low-energy-ion stopping phenomena has been worked out[5], and it became even more interesting to extend the measurements not only to small energies but also to other ions and other gases.

2. Experimental techniques

The principle of the method was the same as in our previous experiment[1]. The ions were stopped in a gas; the gas volume was located between two parallel plates and the stopped ions were collected on one of the plates by a transverse electric field. Radioactive ions were used, and the activity

distribution on the plate gave directly the range distribution. In fact, in favourable experiments, a two-dimensional activity distribution, giving information also on the scattering, was obtained.

The measuring chamber is shown in fig. 1. 50 keV ions were produced by means of the Copenhagen isotope separator. Some of the ions entered the chamber through a narrow slit between two steel plates pressed against a teflon disk; a hole in the teflon determined the length of the slit (1 mm),

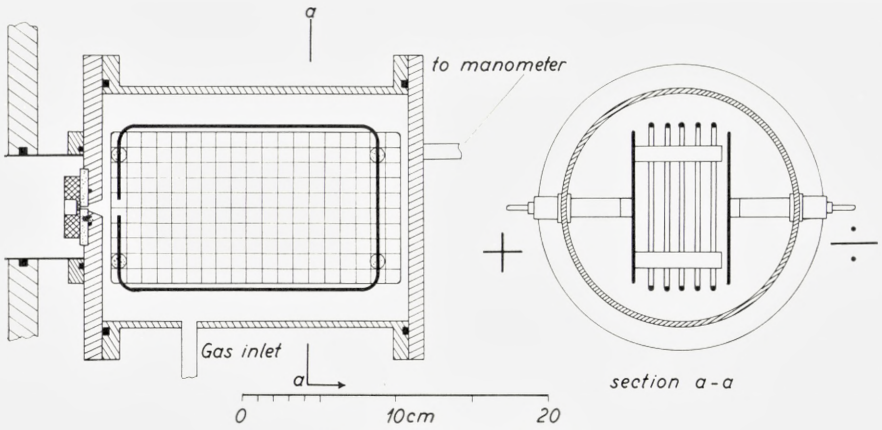

Fig. 1. Stopping chamber.

whereas the width was determined by the distance between the steel plates, which was 0.01–0.05 mm, different for different gases and ions. At the place of the slit the steel plates were 2 mm thick; in order to enable the ion beam to penetrate through the slit, the latter had to be oriented in the proper direction; this could be done by tilting the whole chamber. The chamber was filled with a pure gas to a suitable pressure, 0.5–6 mm Hg, which was measured by means of a calibrated manometer filled with Apiezon B oil. The gas continuously leaked out into the separator vacuum through the slit; new gas was admitted from a storage tank through a needle valve, and the pressure in the measuring chamber was kept constant within $\pm 2\,\%$, or better in favourable cases.

The electric field was applied between two brass plates, $10 \times 19\ \mathrm{cm}^2$, held parallel to each other at a distance of 4–9 cm, varying for different experiments. Each of the plates was supported by two teflon insulators, and one was held at a positive, the other at a negative potential with respect to the chamber wall. The voltages were ± 220 V or less, and it is easily seen

that the path of the ions is hardly influenced by the electric field as long as they are not stopped down to thermal velocities. Rings of 1.5 mm copper wire, spaced one centimeter and held at the appropriate potentials, were used to improve the homogeneity of the field. In contrast to our earlier measurements[1]), the present investigations were probably not disturbed by space charges in the gas volume. In this connection, it may be noted that the role of the isotope separator is not only that it produces and accelerates the ions, but the actual mass separation is also highly important. When measuring the range of Na^{24} ions, for example, the strong beam of the carrier Na^{23} does not enter the measuring chamber; if it did, one might fear that space charges would distort the field and that, therefore, the activity distribution on the plate would not correspond to the actual distribution of the end-points of the ion paths.

The ions coming from the separator are positively charged. Experience shows that, in some gases and for some ion types, most of them also have a positive charge when they are stopped down to thermal velocities. This is the basis for the method. It may be important that the electrons produced by ionization are quickly removed from the gas volume; for this reason, attempts were made to use pure gases in which no electron attachment would take place. For all gases except helium the storage tank was provided with a purifier with hot calcium, through which the gas was continuously circulated; when helium was used, it was passed through charcoal in liquid air.

Of course, the purity of the gas is also important because the range varies from gas to gas. It is especially important for the light gases, because here the ranges are much longer than in the heavier gases (as measured in cm NTP). Assuming the components of a gas mixture to act independent of each other in the stopping process, and assuming a velocity independent stopping power, one finds that an impurity of n percent of nitrogen in hydrogen will cause an error (decrease) in the range of about $6\,n$ percent. The purifier removes electronegative gases such as oxygen and water vapor, but not nitrogen; therefore, the tightness of the apparatus was thoroughly investigated before each run. In a few cases a leak developed in the gas inlet tubing, and a much too small value for the hydrogen range was obtained; at the same time, the form of the activity distribution showed that something was wrong. The measurements in hydrogen were repeated, often with long time intervals, and it is believed to be extremely improbable that impurities should have caused significant errors. For Na^{24} and Ga^{66} more than $99\,\%$ of the ions are collected on the negative plate, when hydrogen

or deuterium is the filling gas. The ranges in these two gases were measured in experiments made immediately after each other; in between, the apparatus was not touched except for the inversion of the field and the necessary operation of some stopcocks and the needle valve to change from hydrogen to deuterium, so that one plate gave the hydrogen distribution, the other the deuterium distribution.

The collector plates were covered with 3 mg/cm^2 aluminium foils, which were cut into pieces 1×1 cm^2; each piece could be placed in its own little specimen tube, and the γ-activity was measured by means of a 3×3 inch NaJ-crystal in a well screened set-up with a low background. In some experiments smaller units 0.5×0.5 cm^2 were used; instead of the foil method another technique was employed, the activity being collected on the end faces of many small aluminium blocks, $0.5 \times 0.5 \times 1.0$ cm^3, screwed together in such a way as to give a smooth collector surface.

Measurements were made on Na^{24}, Ga^{66} and Au^{198} ions. Activities of the order of 100 mC were needed; in these experiments the ion separator beam normally had a cross section of about 0.2 cm^2, the transmission through the entrance slit of the measuring chamber thus being about 10^{-3}; the separator efficiency was about 0.01–0.05. Ga^{66} was produced by bombarding copper with 20 MeV α-particles from the Copenhagen cyclotron. The activity was scraped off the copper target, carriers were added, and copper and zink were chemically removed. Galliumoxid was produced, and in the ion source of the separator it was transformed into galliumchlorid by addition of CCl_4 [6]. Gold and the chloride of sodium were bombarded with neutrons in the Danish reactor DR2 at Risø and subsequently, without further treatment, placed into the ion source oven.

3. Results. Discussion of particle charge and collection

3.1. Ga^{66} ions

Figs. 2 and 3 show the activity distributions on the negative plate when the stopping gas was hydrogen and nitrogen, respectively. In the light gases the range is sharply defined, and the scattering is small; in the heavier gases the straggling and scattering give considerably broader distributions, both lengthwise and sidewise.

In fig. 4 the range distributions in hydrogen and deuterium are shown. A whole row of the aluminium blocks were counted simultaneously; i. e. the ordinates give the activities on 0.5 cm wide strips of the plate perpendicular to the original beam direction (when this is taken as X-axis: $\Delta x = 0.5$

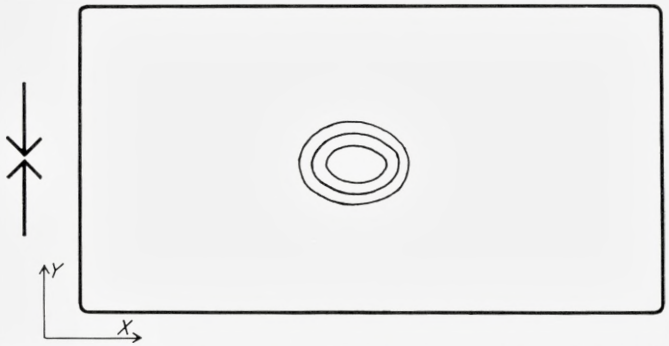

Fig. 2. Distribution of Ga^{66} activity on the negative collector plate, when hydrogen at a pressure of 3.1 mm Hg is used as stopping gas. The lines are drawn through points corresponding to 75 %, 50 % and 25 % of the maximum density of activity.

cm, $\Delta y = 4$ cm). Except for a very small tail on the left side of the hydrogen peak, the distributions are Gaussian.

Fig. 5 gives the range distribution in nitrogen. 96 % of the activity were found on the negative plate, and the activity distribution on this plate may safely be taken as a good picture of the range distribution. It is not Gaussian; since it is unsymmetric, we may distinguish between the most probable range R_p and the mean range R_m.

The activity distribution on the positive plate is not so well determined, because the activity was too small. It seems to be more symmetric; the mean range S_m for these ions is almost equal to R_m, maybe slightly longer. Probably a small part of the particles are neutralized near the end of their paths, and after being stopped down to thermal velocities by nuclear collisions they diffuse around, some of them ultimately reaching the positive, some the negative plate. Since in this diffusion process they move more or less

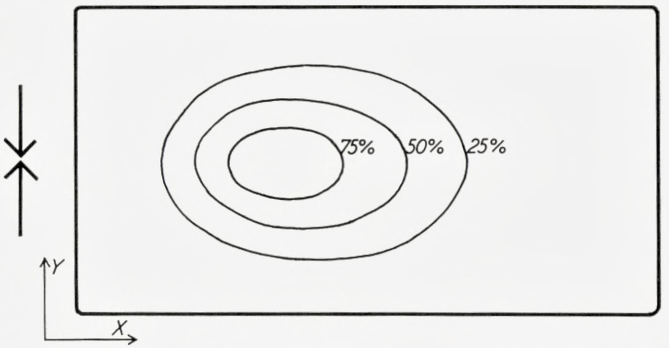

Fig. 3. The same as fig. 2 with nitrogen at a pressure of 0.56 mm Hg.

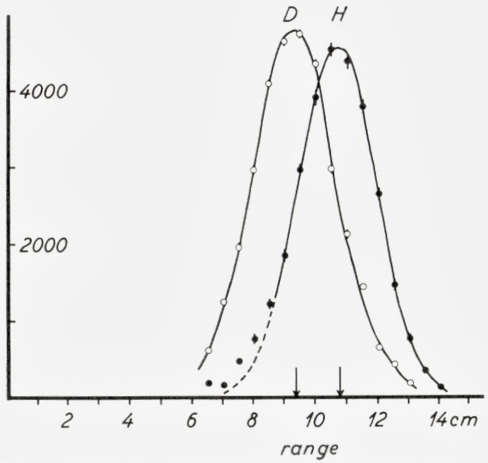

Fig. 4. Range distribution of Ga^{66} ions in hydrogen and deuterium for a pressure of 3.1 mm Hg. The curves are Gaussian, fitted to the points.

isotropically in all directions, the distribution on the positive plate should be smeared out as compared to the actual range distribution, but the mean range should not be much affected. If the neutralization takes place at some distance from the end of their paths, they might have a longer range than the not neutralized ions. However, it should be considered that the travelling particles probably undergo many charge exchange processes and, consequently, it does not seem reasonable to talk about two types of ions— neutrale and positive—as long as they move with velocities at which reversible charge exchanges may occur. Apparently most of the particles are or become positive at the very end of the track, but a few fail to do so.

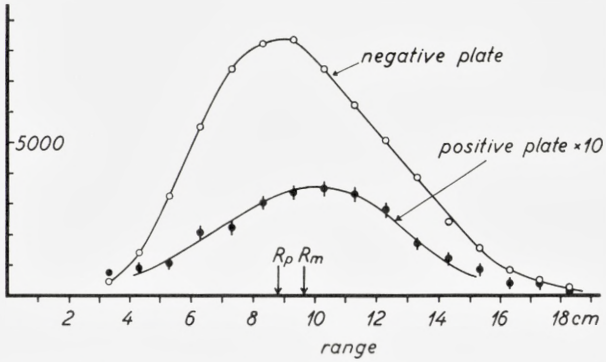

Fig. 5. Range distribution of Ga^{66} ions in nitrogen. Pressure 0.56 mm Hg.

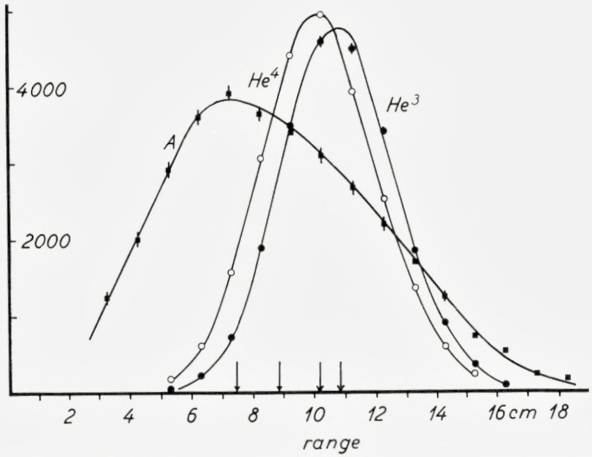

Fig. 6. Range distributions of Ga^{66} ions in He^3, He^4 and A. The curves for He^3 and He^4 refer to the same pressure, 2.95 mm Hg, whereas the argon pressure was 0.60 mm Hg. The two helium curves are Gaussian. For A the figures on the activity axis should be reduced by a factor of two. Arrows indicate: R_p for A, R_m for A, R_p for He^4 and R_p for He^3.

If this explanation is true, the same amount of neutral particles must reach the negative plate. A correction to the range distribution curve would therefore be appropriate; because of the smallness it has been neglected. The distribution on the positive plate should be expected to be broader than that on the negative plate, but this is hardly confirmed by the experiments. The half-widths of the lengthwise distributions are nearly equal, and the same is valid for the transversal distributions (see table 1) when the latter are determined by measuring the activity across a 6 cm wide strip ($\Delta x = 6$, $\Delta y = 1$).

Fig. 6 shows the range distributions in He^3, He^4 and A. In the helium gases the distributions are Gaussian; all activity was found on the negative plate. In argon the distribution is more unsymmetric than in nitrogen; about 10 % of the activity was collected on the positive plate, but the distribution was not measured.

3.2. Au^{198} ions

In hydrogen about 25 % of the Au^{198} activity was found on the positive plate. In this case a difference between the distributions on the two plates was found (see fig. 7), which clearly points at the above proposed explanation for the activity on the positive plate: Some particles are neutral when stopped, and they produce by diffusion a broad range distribution on both

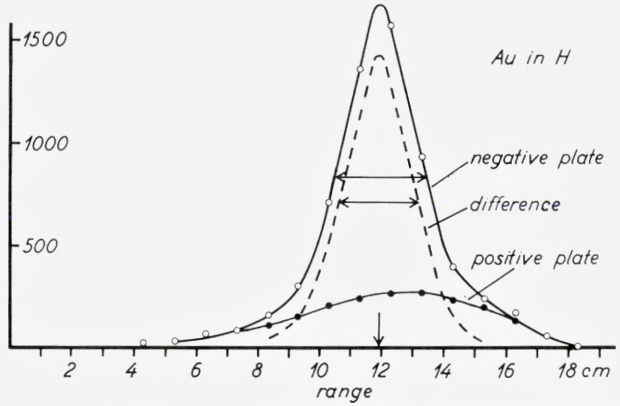

Fig. 7. Distribution of Au^{198} activity on the negative and positive collector plates with hydrogen at 2.9 mm Hg. The difference is assumed to give the range distribution, see text.

plates. This distribution is directly observed on the positive plate; on the negative plate it appears as the "wings" on the much sharper distribution produced by the positive ions. The same difference was found in the transversal distributions, and very similar results were obtained in deuterium (see fig. 8). Consequently, the difference between the activity distributions on the negative and positive plate may be assumed to give the best picture of the true distribution of the particle end-points.

In neon the range distribution is broader and slightly unsymmetric; about 20 % of the activity was found on the positive plate, but it was too small to permit a measurement of the distribution.

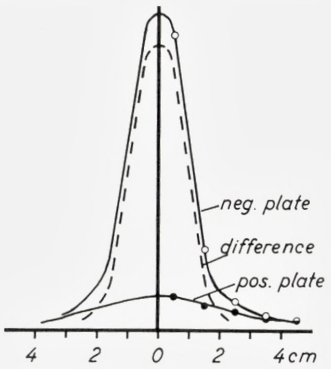

Fig. 8. Distribution of Au^{198} activity across the negative and positive collector plates with deuterium at 2.4 mm Hg. The distributions were assumed to be symmetric. For symmetrically placed aluminium foils only the activity sum was measured.

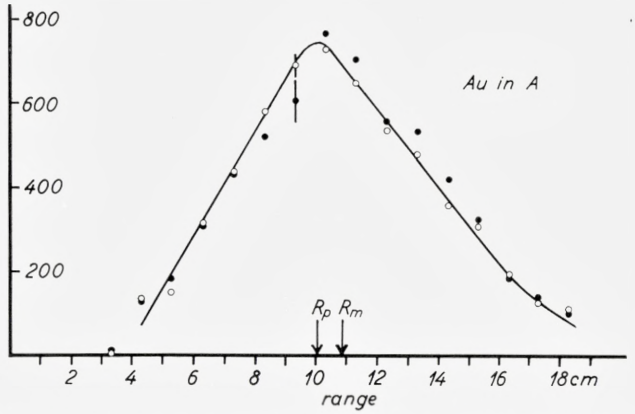

Fig. 9. Distribution of Au^{198} activity along the negative and positive collector plates with argon at 0.38 mm Hg. Open circles correspond to the negative plate; full circles to the activity on the positive plate multiplied by 1.6.

Fig. 9 shows the distributions in range obtained in argon. The activity was divided between the two plates in the ratio 62:38; the range distributions as well as the transversal distributions were almost equally shaped on the two plates. This may indicate that the particles at the end-points of their paths appear in positive, negative and neutral states.

3.3. Na^{24} ions

In hydrogen and deuterium all activity was found on the negative plate; the range distributions were Gaussian. In neon a slight asymmetry was observed, and about 20 % of the particles went to the positive plate.

The range distributions on the two plates obtained in argon are shown in fig. 10. In this case the distribution on the positive plate is the narrower, and we cannot explain things as simple as for Au^{198} ions in the light gases. It has to be taken into account that the experimental conditions are not the very best in this case, since, due to the large straggling and scattering, the activity is distributed over the entire area of the collector plates (see figs. 10 and 11). A small part of the particles may reach the collector plates before being thermalized; the narrower distribution on the positive plate may in part be caused by such particles. In fact, if we consider particles with end-points at a certain distance T from the median plane, their range distribution is the narrower, the larger T is. In fig. 10 the open squares give the range distribution as measured for the middle four centimeters ($\Delta x = 1$, $\Delta y = 4$); by including also the outermost three centimeters on both sides

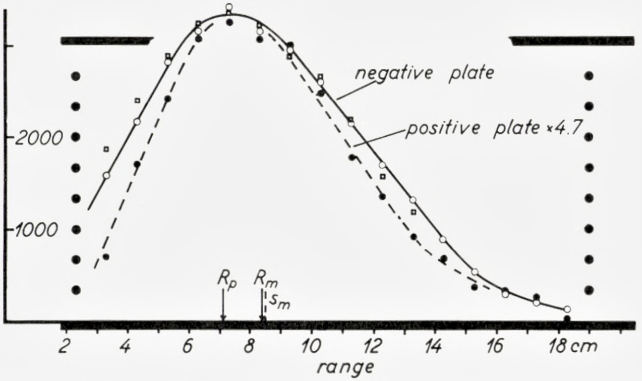

Fig. 10. Distribution of Na^{24} activity along the collector plates with argon at 1.7 mm Hg. Full circles correspond to the positive plate (the activity being multiplied by 4.7); open circles and squares to the negative plate. Squares are measured with $\Delta y = 4$ cm, circles with $\Delta y = 10$ cm. The figure also shows the geometry of the collector plates and the grid wires.

one obtains the narrower distribution given by the open circles ($\Delta x = 1$, $\Delta y = 10$). However, if the activity on the positive plate were caused only by particles striking it before being thermalized, the negative plate would receive the same number of particles in flight. That would correspond to 32 % of the particles striking the plates and, judging from figs. 10 and 11, this number seems completely unreasonable. Probably some particles are neutral at the end of their paths; now those particles lying close to one of the plates (with large T values) will have a higher chance of reaching this plate by diffusion than particles lying farther away (f. ex. with $T = 0$). This is another effect tending to give a narrower distribution on the positive than on the negative plate.

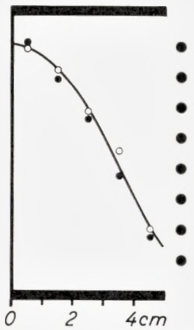

Fig. 11. Transversal distribution of Na^{24} activity with argon in the chamber. Measured with $\Delta x = 4$ cm and with x-values corresponding to the position of the peak in the lengthwise distribution in fig. 10. Again the geometry is shown. The experimental points represent the activity sum of symmetrically placed aluminium foils like in fig. 8.

3.4. Summary of results

The experimental results are summarized in table 1. Here R_p is the most probable range as determined from the activity distribution on the negative plate. R_m is the mean range from the same distribution, ΔR and ΔT are the half-widths of the lengthwise and crosswise distributions on the same plate. ΔR refers to measurements in which $\Delta x = 1$ cm, $\Delta y = 8$ cm (except for Ga ions in hydrogen and deuterium, where $\Delta x = \frac{1}{2}$ cm, $\Delta y = \frac{8}{2}$ cm). ΔT refers to measurements with $\Delta y = 1$ cm, $\Delta x \sim 6$ cm, taken for x-values around the peak in the R-distribution. "Int." is the activity found on the positive plate, in percent of the total activity found on both plates; if it is ascribed to neutral particles, the same number will have diffused to the negative plate and some will have escaped through the grid to the chamber walls. S_m, ΔR^+ and ΔT^+ have similar meanings as R_m, ΔR and ΔT, but they refer to the activity distribution on the positive plate.

TABLE 1. Experimental results

		Negative Collector Plate				Positive Collector Plate			
		R_p $\mu g/cm^2$	R_m/R_p %	$\Delta R/R_p$ %	$\Delta T/R_p$ %	Int. %	S_m/R_p %	$\Delta R^+/R_p$ %	$\Delta T^+/R_p$ %
Na^{24}	H_2	7.51	100	39	25	< 1	..	..	..
	D_2	17.9	100	47	28	< 1	..	..	..
	Ne	21.2	103	93	60	~ 20	..	..	..
	A	26.9	117	122	100	16[1]	118	100	95
Ga^{66}	H_2	3.64	100	27	17	< 3	..	..	..
	D_2	6.45	100	33	20	..	..	..	..
	He^3	5.25	100	40	26	..	..	..	..
	He^4	6.70	100	44	28	< 2	..	..	..
	N_2	7.5	110	82	55	4	112	88	56
	A	9.8	117	115	75	~ 10	..	..	..
Au^{198}	H_2	3.74	100	18[2, 3]	15[2, 3]	25	104	60	40
	D_2	6.25	100	18[2, 3]	15[2, 3]	20	104	75	45
	Ne	7.20	103	48	..	15–20	..	..	..
	A	8.20	109	75	55	38	110	75	55

[1] A small part of this activity may be due to particles reaching the positive collector plate before being thermalized.

[2] Figures obtained from the difference between the activity distributions on the negative and positive plate.

[3] Corrected for influence of finite width of aluminium pieces.

In some cases, indicated in the table, where the measured half-widths are small, the finite widths of the aluminium pieces justified a correction. For example, one finds that a Gaussian with a true half-width $\Delta R/R = 15\,\%$ will give a measured half-width of $18\,\%$ when $\Delta x/R = 0.1$, Δx being the length of the aluminium pieces.

4. Discussion

4.1. Shapes of the range distributions

The difference in shape of the range distributions in the light and heavy gases is a most conspicuous result. In hydrogen and helium the distributions are Gaussian, but in the heavier gases they exhibit an increasing skewness. For these rather low velocity ions the stopping is mainly caused by nuclear collisions and the difference in straggling is related to the magnitude of the energy loss in single encounters. The maximum energy transfer is

$$T_m = \frac{4\,M_1 M_2}{(M_1+M_2)^2} \cdot E = \gamma E, \tag{1}$$

where E is the energy, M_1 and M_2 are the mass numbers of the incoming and the struck nucleus, respectively. Although the average energy loss per collision is much smaller, we may expect some correlation between γ and the skewness. In table 2 the values of γ are shown; comparing these values with the values for R_m/R_p from table 1 we note the similarity between gold ions in argon and gallium ions in nitrogen, as well as between sodium and gallium ions in argon. Actually, the latter result, the same values for R_m/R_p for sodium and gallium ions in argon, is rather surprising,

TABLE 2. Maximum fractional energy transfer, γ

	Na^{24}	Ga^{66}	Au^{198}
H^1	0.154	0.059	0.020
D^2	0.28	0.114	0.040
He^3	..	0.17	..
He^4	..	0.22	..
N^{14}	..	0.58	..
Ne^{20}	0.99	..	0.33
A^{40}	0.94	0.94	0.56

since we may expect some difference between cases with $M_2 > M_1$ and those with $M_2 < M_1$ [7]. In fact, for sodium ions the skewness is small both in neon and in argon; this may indicate the influence of electronic stopping.

4.2. Range straggling.

For pure nuclear stopping LINDHARD and SCHARFF give the formula

$$\left(\frac{\sigma'}{R'_m}\right)^2 = \frac{1}{6}\,\gamma, \tag{2}$$

where σ' is the fluctuation in path length and R'_m is the mean length measured along the actual path. This expression results, when a potential proportional to r^{-2} is assumed between the colliding particles, but it should give a good approximation also for somewhat different exponents in the potential. LINDHARD, SCHARFF and SCHIØTT[5] (in the following cited as LSS) have assumed, as a better approximation, a potential of the form $r^{-1}\cdot\varphi_0(r/a)$, where φ_0 is the Fermi function, and the screening parameter is given by

$$a = \frac{\hbar^2}{me^2}\cdot 0.8853\,(Z_1^{2/3}+Z_2^{2/3})^{-1/2}, \tag{3}$$

m being the electronic mass, Z_1 and Z_2 the nuclear charge numbers of the incoming and the struck particle, respectively. They also take into account the influence of electronic stopping, assuming the contribution to the straggling from electronic collisions to be negligible. Their results are given in graphs (LSS fig. 6) showing $\frac{1}{\gamma}\left(\frac{\sigma'}{R'_m}\right)^2$ plotted against a dimensionless energy parameter ε defined by

$$\varepsilon = E\,a\,\frac{M_2}{Z_1 Z_2\,e^2(M_1+M_2)}. \tag{4}$$

Furthermore, they use a dimensionless range parameter

$$\varrho = R'N M_2\,4\pi\,a^2\,\frac{M_1}{(M_1+M_2)^2}, \tag{5}$$

where N is the number of stopping atoms per cm^3. In these units the electronic stopping is supposed to be given by

$$\frac{d\varepsilon}{d\varrho} = k\cdot\varepsilon^{1/2} \tag{6}$$

with

$$k = Z_1^{1/6} \frac{0.0793\, Z_1^{1/2} Z_2^{1/2} (M_1 + M_2)^{3/2}}{(Z_1^{2/3} + Z_2^{2/3})^{3/4} M_1^{3/2} M_2^{1/2}} . \tag{7}$$

The values of ε and k calculated according to (4) and (7) are given in table 3, which also gives the ratio R'/R between the path length and the (projected) range. This ratio is found from the graphs in LSS, figs. 8 and 9, and the values are slightly different from those which would be obtained from the approximate formula[4)]

$$R' = R\left(1 + \frac{1}{3}\frac{M_2}{M_1}\right). \tag{8}$$

By means of the ratio R'/R and the values given in table 1 we obtain the figures which in table 3 are denoted "experimental" for the quantity σ/R'_m, where $\sigma = \Delta R/2.34$. For comparison, the theoretical values for σ'/R'_m denoted "LSS_{n+e}" and obtained from LSS fig. 6, are given. In the last column, values corresponding to pure nuclear stopping and obtained from the same graphs, LSS fig. 6, are tabulated.

We do not know the exact relation between σ and σ'. This is unimportant for the light gases, where R and R' are nearly the same and where one may

TABLE 3.

		ε	k	R'/R	σ/R'_m "exp."	σ'/R'_m LSS_{n+e}	σ'/R'_m LSS_n
Na^{24} $V = 0.29\ V_0$	H	2.42	0.11	1.01	0.17	0.12	0.15
	D	4.66	0.08	1.03	0.19	0.15	0.20
	Ne	2.18	0.13	1.25	0.31	0.30	0.39
	A	1.49	0.18	1.51	0.29	0.29	0.38
Ga^{66} $V = 0.18\ V_0$	H	0.237	0.13	1.00	0.12	0.08	0.09
	D	0.467	0.10	1.01	0.14	0.12	0.13
	He^3	0.337	0.11	1.02	0.17	0.14	0.16
	He^4	0.443	0.10	1.02	0.18	0.16	0.18
	N	0.356	0.11	1.08	0.29	0.27	0.29
	A	0.269	0.13	1.25	0.33	0.34	0.36
Au^{198} $V = 0.10\ V_0$	H	0.0234	0.16	1.00	0.08	0.05	0.05
	D	0.0468	0.11	1.00	0.08	0.07	0.07
	Ne	0.0396	0.11	1.04	0.19	0.20	0.21
	A	0.0383	0.11	1.08	0.27	0.26	0.27

also put $\sigma = \sigma'$. LSS have calculated the ratio σ'/σ for $M_1 = M_2$ and for pure nuclear scattering corresponding to a potential r^{-s} with $\frac{3}{2} < s < 3$. This ratio is smaller than the ratio R'/R, and possibly the influence of electronic stopping will make it still smaller. We may, as a first approximation, assume $\sigma' \approx \sigma$ and therefore we should expect our "experimental" values for σ/R'_m and the theoretical values $\mathrm{LSS_{n+e}}$ for σ'/R'_m to be nearly the same. In fact, the agreement is very close for the heavy gases. It may be noted that the experimental values for Na^{24} ions in neon and argon are consistent with the theory, according to which the electronic stopping is appreciable even for such small velocities.

For the light gases the experimental values for the straggling are larger than the theoretical ones. Of course we cannot feel quite sure that the thermalized ions follow exactly the electric field lines, or that the experimental distributions are not broadened for some other unknown reasons. However, the theoretical estimates are only approximate, and since they are based on the Thomas-Fermi model of the atom, the approximation may be better for the heavy than for the light gases.

4.3. Transversal Distributions

The scattering is small in the light gases, and it increases with increasing Z_2 roughly proportional to the range straggling. The maximum fractional transverse momentum transfer is $M_2/(M_1+M_2)$, and we might look for a possible correlation between this quantity and the width of the transverse distribution. For this purpose values of $\sigma_T \sqrt{(M_1+M_2)/M_2}/R_m$ are given in table 4, σ_T being the measured half-width divided by 2.34.

TABLE 4. $\sigma_T \sqrt{(M_1+M_2)/M_2}/R_m$

	Na^{24}	Ga^{66}	Au^{198}
H	0.54	0.59	0.90
D	0.43	0.50	0.64
He^3	..	0.53	..
He^4	..	0.50	..
N	..	0.51	..
Ne	0.37	..	..
A	0.46	0.45	0.52

It may be seen from table 4, that the values are of the order of 0.5, except for gold ions in the light gases. In just these cases the values are somewhat uncertain, since there are considerable corrections from neutral particles. Other errors, such as angular width of the incoming beam from the separator and the scattering in the entrance slit, may possibly also play a role for these narrow distributions. However, it may be expected that σ_T also depends on the charge numbers Z_1 and Z_2.

4.4. Comparison of the range values with theory

From the experimental mean ranges R_m given in table 1 we find the mean path lengths R'_m by means of the values for R'/R in table 3. Next, from R'_m the corresponding values of ϱ_m are calculated according to formula (5). Furthermore, using the ε- and k-values from table 3 and the graphs LSS figs. 3, 4, 12 and 13, we obtain theoretical values for ϱ_m. The results are given in table 5.

TABLE 5. The reduced mean range ϱ_m

	Na^{24}			Ga^{66}			Au^{198}		
	"exp."	theor.	$\frac{\text{theor.}}{\text{exp.}}$	"exp."	theor.	$\frac{\text{theor.}}{\text{exp.}}$	"exp."	theor.	$\frac{\text{theor.}}{\text{exp.}}$
H	8.1	5.5	0.68	0.82	0.66	0.80	0.160	0.128	0.80
D	18.3	11.7	0.64	1.42	1.17	0.83	0.264	0.204	0.77
He^3	..	..	..	1.07	0.88	0.82	..	..	..
He^4	..	..	..	1.34	1.14	0.86	..	..	..
N	..	..	..	1.13	0.89	0.79	..	..	..
Ne	5.8	4.7	0.81	..	..	..	0.231	0.182	0.79
A	3.9	3.1	0.80	0.83	0.62	0.75	0.222	0.180	0.81

It will be seen that the variation of the ϱ-values with ε predicted by the theory is well reproduced by the experiments. The theoretical values are all lower than the experimental ones, on an average about 20 %. We estimate the uncertainty in the experimental values to be 3 %, not including the uncertainty in R'/R. One can imagine several systematic errors, all giving too *small* experimental ranges, but we hope to have avoided them.

4.5. Ranges in isotopic stopping media

As already mentioned in the Introduction, measurements in isotopic stopping media may be of special interest, since range differences in such materials must be due entirely to nuclear stopping. Table 6 gives the ratio

R_D/R_H of the range in deuterium and hydrogen for three kinds of incoming particles and the ratio R_{He^4}/R_{He^3} for Ga^{66} ions (range in cm). It may be seen that, for the rather slow 50 keV gallium ions, the range is shorter in deuterium than in hydrogen, opposite to what was found for somewhat faster gallium ions[1]. For the still slower 50 keV gold ions the deuterium range is still shorter as compared to the hydrogen range, whereas for the slightly faster 50 keV sodium ions the range in deuterium is the longer. This peculiar behaviour shows that the nuclear stopping is sometimes larger, sometimes smaller in deuterium than in hydrogen. That the theory is able to account for this phenomenon may be seen already from table 5, but in order to facilitate a comparison, we have in table 6 given also the theoretical values. The experimental and theoretical values agree within the limits of error.

TABLE 6. Range ratios for 50 keV ions

	R_D/R_H		R_{He^4}/R_{He^3}	
	exp.	theor.	exp.	theor.
Na^{24}	1.19	1.15	..	..
Ga^{66}	0.89	0.92	0.96	1.00
Au^{198}	0.84	0.80	..	..

According to LSS, the nuclear stopping cross section for $M_1 \gg M_2$ is proportional to $M_2^{1-2/s}$, when the effective potential in the collisions is proportional to r^{-s}. Fast ions are able to approach each other closely; then, the potential resembles the pure Coulomb potential r^{-1}, and for such ions deuterium has the smaller nuclear stopping cross section and hence the longer range. For slow ions the distance of closest approach is larger, and s is increased. For $s > 2$, deuterium will have the higher stopping power. According to LSS, the shift should take place for ε-values slightly smaller than 0.5; this is confirmed by the experimental results.

4.6. Other experimental range measurements

To our knowledge, there are no other measurements with the same projectiles, the same energy and the same stopping gases. There are many measurements with somewhat similar projectiles etc. (see for instance [8] [9] for summaries). However, a direct comparison is difficult; instead, one can compare the various experimental results with the theory of LSS, see ref. [5].

We wish to thank PH. DAM, techn. eng., for help in the production of Ga^{66} in the cyclotron and MOGENS JØRGENSEN, M. Sc. Chem. Eng., for the chemical treatment of the bombarded target. Furthermore, we gratefully acknowledge the assistance of Mr. H. CHRISTENSEN in cutting the foils, and counting.

References

1. LISE BRYDE, N. O. LASSEN and N. O. ROY POULSEN: Mat. Fys. Medd. Dan. Vid. Selsk. **33**, no. 8, 1962.
2. J. LINDHARD and M. SCHARFF: Private communication.
3. B. G. HARVEY, P. F. DONOVAN, J. R. MORTON and E. W. VALYOCSIK: U.C.R.L. 8618, p. 17, 1959.
4. J. LINDHARD and M. SCHARFF: Phys. Rev. **124**, 128, 1961.
5. J. LINDHARD, M. SCHARFF and H. E. SCHIØTT. Mat. Fys. Medd. Dan. Vid. Selsk. **33**, no. 14, 1963. In the present paper cited as LSS.
6. G. SIDENIUS and O. SKILBREID: E. M. Separations with High Efficiency of Microgramme Quantities. In: E. M. Separation of Radioactive Isotopes. Springer Verlag, Wien 1961.
7. K. O. NIELSEN: Electromagnetically Enriched Isotopes and Mass Spectroscopy. Butterworth Scientific Publications, London 1956, p. 68.
8. S. K. ALLISON and M. GARCIA MUNOZ: Reports National Academy of Sciences, National Research Council, Washington D. C., April 1962.
9. B. G. HARVEY: Ann. Rev. Nucl. Sci. **10**, 235, 1960.

Indleveret til Selskabet den 7. februar 1964.
Færdig fra trykkeriet den 11. juni 1964.